



Alexandria University
Alexandria Engineering Journal

www.elsevier.com/locate/aej
www.sciencedirect.com



Novel idea about the peristaltic flow of heated Newtonian fluid in elliptic duct having ciliated walls

L.B. McCash^a, Sohail Nadeem^{b,*}, Salman Akhtar^b, Anber Saleem^c,
 Salman Saleem^d, Alibek Issakhov^e

^a School of Mathematics & Actuarial Science, University of Leicester, Leicester LE1 7RH, UK

^b Department of Mathematics, Quaid-i-Azam University 45320, Islamabad 44000, Pakistan

^c Department of Anatomy, School of Dentistry, Shaheed Zulfiqar Ali Bhutto Medical University Islamabad, Pakistan

^d Department of Mathematics, College of Sciences, King Khalid University, Abha, Saudi Arabia

^e Al-Farabi Kazakh National University, Faculty of Mechanics and Mathematics, av. al-Farabi 71, Almaty, Kazakhstan

Received 31 May 2021; revised 29 June 2021; accepted 25 July 2021

KEYWORDS

Elliptic duct;
 Cilia;
 Peristalsis;
 Heated fluid;
 Exact solutions

Abstract This novel investigation unfolds the mathematical model of peristaltic flow in an elliptic duct having ciliated walls. The current assessment is carried out by considering a heated Newtonian viscous fluid in this ciliated elliptic duct. A detailed heat transfer study combined with various physical aspects of peristalsis is provided. We have incorporated the appropriate and useful transformations that simplify this mathematical problem into its non-dimensional form with relevant non-dimensional boundary conditions over the surface of ciliated elliptic duct. Finally, the exact mathematical results are computed for this interesting problem. A thorough graphical assessment is also included for a complete understanding of mathematical results. The axially symmetric flow behaviour is noted for both velocity and temperature profiles in this elliptic duct having ciliated walls.

© 2021 THE AUTHORS. Published by Elsevier BV on behalf of Faculty of Engineering, Alexandria University. This is an open access article under the CC BY-NC-ND license (<http://creativecommons.org/licenses/by-nc-nd/4.0/>).

1. Introduction

The mechanism of fluid movement inside a duct having deformable sinusoidal walls is termed as Peristalsis. These systematically contracting and relaxing walls of duct move the fluid in axial direction. The major engineering and industrial applications of this peristaltic flow phenomenon has made it a very keen topic of interest. Some industrial applications of

peristalsis involve the shifting of some fluids like noxious, corrosive, slurry and aggressive chemicals etc. There are many physiological applications as well that include food displacement in digestive tract, blood circulation that involve small scale vessels and urine movement etc [1]. The problems of peristaltic flow phenomenon are being studied by many researchers due to its applicability. Barton and Raynor [2] had disclosed a mathematical study that addresses the topic of peristaltic movement in tubes. Pozrikidis [3] had interpreted mathematically the two-dimensional flow inside a channel having deformable sinusoidal walls. Siddiqui and Schwarz [4] had provided the mathematical model that discloses the axis-symmetry flow of a non-Newtonian fluid across a geometry having sinusoidal

* Corresponding author.

E-mail address: sohail@qau.edu.pk (S. Nadeem).

Peer review under responsibility of Faculty of Engineering, Alexandria University.

<https://doi.org/10.1016/j.aej.2021.07.035>

1110-0168 © 2021 THE AUTHORS. Published by Elsevier BV on behalf of Faculty of Engineering, Alexandria University.

This is an open access article under the CC BY-NC-ND license (<http://creativecommons.org/licenses/by-nc-nd/4.0/>).

Nomenclature

$(\bar{X}, \bar{Y}, \bar{Z})$	Cartesian coordinate system	\underline{d}	Wave amplitude
a_0, b_0	Ellipse half axes ($b_0 < a_0$)	T_w	Duct's wall temperature
λ	wavelength	D_h	Hydraulic diameter of ellipse
c	Velocity of propagation	\underline{k}	Thermal conductivity
μ	viscosity	T_b	Bulk temperature
C_p	Heat capacity	δ	Aspect ratio
e	Eccentricity of ellipse	ρ	Density
ϕ	Occlusion (amplitude to radius ratio)	α	Eccentricity of elliptical motion of cilia
B_r	Brickmann number	t	time
β	Wave number for metachronal wave		
$(\bar{U}, \bar{V}, \bar{W})$	Velocity components		

deformable walls. The already available recent literature involves the mathematical models for peristaltic flow that include various geometries like cylinder [5], curved tube [6], asymmetric geometry [7], rectangular duct [8] and elliptic duct [9]. Fig. 1.

In many industrial problems, where space is a salient feature in designing the duct and the main target is a finer cooling result for heat exchanger then an elliptic duct is preferable than circular one [10]. This happens due to a long circumferential length of an elliptic duct than the circumferential length of a circular one even if both have same cross-sectional areas. Abdel Wahid et al. [11] had disclosed an experimental study for the flow of heat with laminar flow properties across an elliptic duct. Maia et al. [12] had presented the mathematical model that interprets the flow of heat inside a duct with elliptic cross-section. Ragueb and Mansouri [13] had examined mathematically the flow of heat with viscous dissipation across an elliptic duct by utilizing numerical approach for solution. Further, some current investigations that interpret the mathematical analysis of flow and heat transfer across elliptic ducts are given [14–16].

The combine mathematical analysis of peristaltic flow and cilia generated metachronal wave is also a topic of huge interest. Cilia are basically threadlike tiny structures (just like hairs) that are attached to the duct surface and their systematic as

well as rhythmic action generates a propagating wave that assists the flow. There are certain physiological flow problems that include the role of cilia like locomotion, food displacement in digestive system, respiration and circulation etc [17]. Blake [18] had investigated mathematically an improved model of the cilia developed flow inside tubes. Akbar and Khan [19] had investigated mathematically the flow of heat and fluid transportation inside a cylindrical tube having ciliated as well as sinusoidal deformable walls. Akbar and Butt [20] had presented a mathematical model that interprets the flow of heat for a non-Newtonian fluid across a tube having ciliated sinusoidal walls. The peristaltic flow analysis combined with ciliated walls effect is mathematically investigated by many researchers by considering distinct geometrical models like asymmetric ciliated channel [21], cylindrical geometry having ciliated walls [22] and curved tube with ciliated walls [23] etc. Further, some of the recent and interesting studies that highlight the significance of peristaltic flow through ciliated geometries are referred as [24–27]. This literature review clearly shows that there is not even a single research article that addresses the important topic of peristaltic flow through an elliptic duct having ciliated walls. Thus our main motivation in this work is to present a mathematical analysis that examines the peristaltic flow of a heated Newtonian viscous fluid through an elliptic duct having ciliated walls.

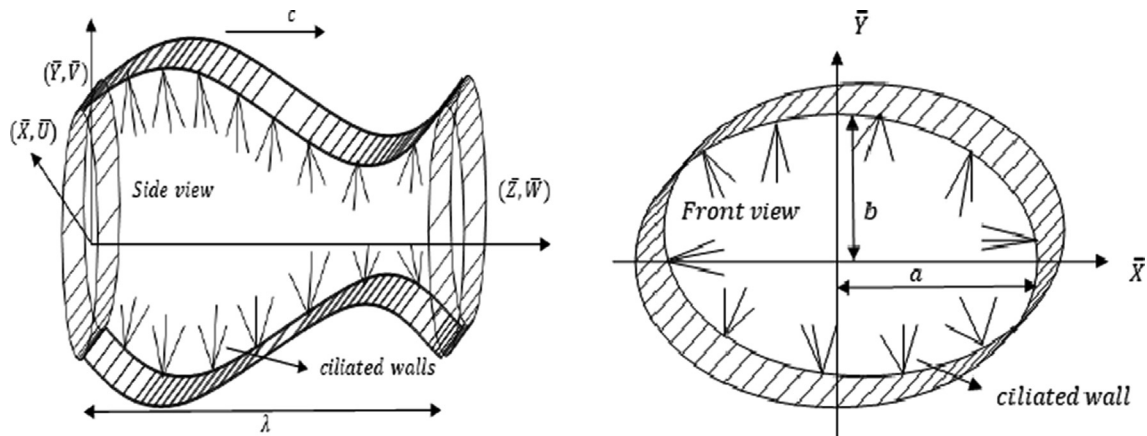


Fig. 1 Side and front view representation of Elliptic duct having ciliated sinusoidal walls. The following mathematical equations represent the envelope model of cilia tips [20].

This work first time introduces a mathematical model for peristaltic flow through an elliptic duct having ciliated walls. The motivation behind our work is to interpret the peristaltic flow mechanism inside a ciliated elliptic duct, since the already available literature work only provides the peristalsis activity for ciliated cylindrical, asymmetric channels etc. The significance of considering an elliptic cross-sectional duct rather than a circular duct is evident from the fact that if we have two different ducts with same cross sectional area, i.e. one circular duct and the other elliptic duct then the elliptic duct will have greater circumferential length as compared to the circular one and it provides a better estimation for heat transfer analysis, finer cooling effects etc. Further, if we consider the biological point of view then we know that cilia exist in different kind of mammals and they play a vital role in many of biological propulsion processes. Moreover, it is not necessary that all the biological structures must have a circular cross-section, for instance it is more appropriate to consider the cross-section of an upper ureter to be elliptic. Also the cross-sectional area alters from a circular to an elliptic one during the contraction of a roller pump. The above highlighted examples point up the physical as well as practical applications of current study. A heated Newtonian viscous fluid is considered to interpret this mathematical problem. Further, a thorough mathematical analysis is presented that explains the vital heat transfer characteristics for the present problem. The various aspects of peristaltic flow mechanism are also taken into account. The developed problem is simplified and reduced to its dimensionless form by applying useful transformations. Finally, the dimensionless mathematical equations are exactly solved according to given dimensionless boundary conditions. In order to facilitate the readers for a deeper understanding of the present problem, we have also elaborated our work by adding a detailed graphical assessment.

2. Mathematical formulation

The present problem is modelled for an elliptic duct with ciliated walls. The geometrical model for an elliptic duct having ciliated sinusoidal walls is given as

$$\begin{aligned} \bar{Y} &= b_0 + b_0 \phi \cos\left(\frac{2\pi}{\lambda}(\bar{Z} - c\bar{t})\right) = \bar{f}(\bar{Z}, \bar{t}), \bar{Z} \\ &= \bar{Z}_0 + b_0 \phi \alpha \sin\left(\frac{2\pi}{\lambda}(\bar{Z} - c\bar{t})\right) = \bar{g}(\bar{Z}, \bar{Z}_0, \bar{t}), \end{aligned} \quad (1)$$

Further, we can represent the axial as well as radial velocities for the cilia tips as follows

$$\begin{aligned} \bar{W} &= \frac{\partial \bar{Z}}{\partial \bar{t}} \Big|_{\bar{Z}_0} = \frac{\partial \bar{g}}{\partial \bar{t}} + \frac{\partial \bar{g}}{\partial \bar{Z}} \frac{\partial \bar{Z}}{\partial \bar{t}} = \frac{\partial \bar{g}}{\partial \bar{t}} + \frac{\partial \bar{g}}{\partial \bar{Z}} \bar{W}, \bar{V} \\ &= \frac{\partial \bar{Y}}{\partial \bar{t}} \Big|_{\bar{Z}_0} = \frac{\partial \bar{f}}{\partial \bar{t}} + \frac{\partial \bar{f}}{\partial \bar{Z}} \frac{\partial \bar{Z}}{\partial \bar{t}} = \frac{\partial \bar{f}}{\partial \bar{t}} + \frac{\partial \bar{f}}{\partial \bar{Z}} \bar{W}, \end{aligned} \quad (2)$$

By combining Eq. (1) and Eq. (2), we get

$$\begin{aligned} \bar{W} &= \frac{-\left(\frac{2\pi}{\lambda}\right) [\phi \alpha b_0 c \cos\left(\frac{2\pi}{\lambda}(\bar{Z} - c\bar{t})\right)]}{\left[1 - \left(\frac{2\pi}{\lambda}\right) \left\{ \phi \alpha b_0 c \cos\left(\frac{2\pi}{\lambda}(\bar{Z} - c\bar{t})\right) \right\}\right]}, \bar{V} \\ &= \frac{\left(\frac{2\pi}{\lambda}\right) [\phi b_0 c \sin\left(\frac{2\pi}{\lambda}(\bar{Z} - c\bar{t})\right)]}{\left[1 - \left(\frac{2\pi}{\lambda}\right) \left\{ \phi \alpha b_0 c \cos\left(\frac{2\pi}{\lambda}(\bar{Z} - c\bar{t})\right) \right\}\right]}, \end{aligned} \quad (3)$$

Here \bar{W} and \bar{V} provide the mathematical expressions for effective as well as recovery strokes of cilia respectively. The movement of cilia tips (shown in Fig. 2) is considered as an elliptical path movement for a complete cycle of effective and recovery strokes. It is evident that the cilium remains rigid during effective stroke while it loosely retreats near the duct surface during its recovery stroke.

The problem is modelled for an incompressible, viscous flow with following mathematical governing equations

$$\frac{\partial \bar{U}}{\partial \bar{X}} + \frac{\partial \bar{V}}{\partial \bar{Y}} + \frac{\partial \bar{W}}{\partial \bar{Z}} = 0, \quad (4)$$

$$\begin{aligned} \rho \left(\frac{\partial \bar{U}}{\partial \bar{t}} + \bar{U} \frac{\partial \bar{U}}{\partial \bar{X}} + \bar{V} \frac{\partial \bar{U}}{\partial \bar{Y}} + \bar{W} \frac{\partial \bar{U}}{\partial \bar{Z}} \right) \\ = -\frac{\partial \bar{P}}{\partial \bar{X}} + \mu \left(\frac{\partial^2 \bar{U}}{\partial \bar{X}^2} + \frac{\partial^2 \bar{U}}{\partial \bar{Y}^2} + \frac{\partial^2 \bar{U}}{\partial \bar{Z}^2} \right), \end{aligned} \quad (5)$$

$$\begin{aligned} \rho \left(\frac{\partial \bar{V}}{\partial \bar{t}} + \bar{U} \frac{\partial \bar{V}}{\partial \bar{X}} + \bar{V} \frac{\partial \bar{V}}{\partial \bar{Y}} + \bar{W} \frac{\partial \bar{V}}{\partial \bar{Z}} \right) \\ = -\frac{\partial \bar{P}}{\partial \bar{Y}} + \mu \left(\frac{\partial^2 \bar{V}}{\partial \bar{X}^2} + \frac{\partial^2 \bar{V}}{\partial \bar{Y}^2} + \frac{\partial^2 \bar{V}}{\partial \bar{Z}^2} \right), \end{aligned} \quad (6)$$

$$\begin{aligned} \rho \left(\frac{\partial \bar{W}}{\partial \bar{t}} + \bar{U} \frac{\partial \bar{W}}{\partial \bar{X}} + \bar{V} \frac{\partial \bar{W}}{\partial \bar{Y}} + \bar{W} \frac{\partial \bar{W}}{\partial \bar{Z}} \right) \\ = -\frac{\partial \bar{P}}{\partial \bar{Z}} + \mu \left(\frac{\partial^2 \bar{W}}{\partial \bar{X}^2} + \frac{\partial^2 \bar{W}}{\partial \bar{Y}^2} + \frac{\partial^2 \bar{W}}{\partial \bar{Z}^2} \right), \end{aligned} \quad (7)$$

$$\begin{aligned} \rho C_p \left(\frac{\partial \bar{T}}{\partial \bar{t}} + \bar{U} \frac{\partial \bar{T}}{\partial \bar{X}} + \bar{V} \frac{\partial \bar{T}}{\partial \bar{Y}} + \bar{W} \frac{\partial \bar{T}}{\partial \bar{Z}} \right) \\ = k \left(\frac{\partial^2 \bar{T}}{\partial \bar{X}^2} + \frac{\partial^2 \bar{T}}{\partial \bar{Y}^2} + \frac{\partial^2 \bar{T}}{\partial \bar{Z}^2} \right) \\ + \mu \left[2 \left\{ \left(\frac{\partial \bar{U}}{\partial \bar{X}} \right)^2 + \left(\frac{\partial \bar{V}}{\partial \bar{Y}} \right)^2 + \left(\frac{\partial \bar{W}}{\partial \bar{Z}} \right)^2 \right\} \right. \\ \left. + \left(\frac{\partial \bar{U}}{\partial \bar{Y}} + \frac{\partial \bar{V}}{\partial \bar{X}} \right)^2 + \left(\frac{\partial \bar{V}}{\partial \bar{Z}} + \frac{\partial \bar{W}}{\partial \bar{Y}} \right)^2 + \left(\frac{\partial \bar{W}}{\partial \bar{X}} + \frac{\partial \bar{U}}{\partial \bar{Z}} \right)^2 \right], \end{aligned} \quad (8)$$

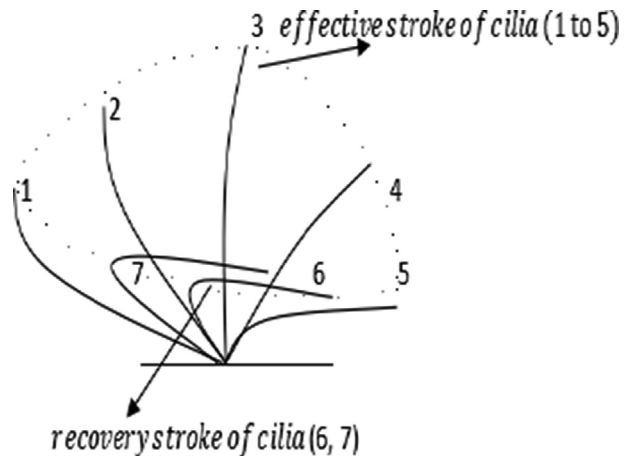


Fig. 2 The motion of a cilium.

The dimensional mathematical form of boundary conditions for an elliptic duct having ciliated walls is

$$\begin{aligned}\bar{W} &= \frac{-(\frac{2\pi}{\lambda})[\phi\alpha b_0 c \text{Cos}(\frac{2\pi}{\lambda}(Z^- - c t^-))]}{[1 - (\frac{2\pi}{\lambda})\{\phi\alpha b_0 c \text{Cos}(\frac{2\pi}{\lambda}(Z^- - c t^-))\}]} \text{ for } \frac{\bar{x}^2}{a^2} + \frac{\bar{y}^2}{b^2} \\ &= 1. \bar{T} = \bar{T}_w \text{ for } \frac{\bar{x}^2}{a^2} + \frac{\bar{y}^2}{b^2} = 1.\end{aligned}\quad (9)$$

The mathematical relation between fixed and moving frame that transfers this problem from an unsteady flow to a steady one is given as

$$\begin{aligned}\bar{x} &= \bar{X}, \bar{y} = \bar{Y}, \bar{z} = \bar{Z} - c t, \bar{p} = \bar{P}, \bar{u} = \bar{U}, \bar{v} = \bar{V}, \bar{w} \\ &= \bar{W} - c,\end{aligned}\quad (10)$$

The non-dimensional variables incorporated in the present study are provided as

$$\begin{aligned}x &= \frac{\bar{x}}{D_h}, y = \frac{\bar{y}}{D_h}, z = \frac{\bar{z}}{\lambda}, t = \frac{c t}{\lambda}, w = \frac{\bar{w}}{c}, p = \frac{D_h^2 \bar{p}}{\mu \lambda c}, \theta \\ &= \frac{\bar{T} - \bar{T}_w}{\bar{T}_b - \bar{T}_w}, \delta = \frac{b_0}{a_0}, \phi = \frac{d}{b_0}, u = \frac{\lambda \bar{u}}{D_h c}, v = \frac{\lambda \bar{v}}{D_h c}, a \\ &= \frac{\bar{a}}{D_h}, b = \frac{\bar{b}}{D_h}, B_r = \frac{\mu c^2}{k(\bar{T}_b - \bar{T}_w)}, \beta = \frac{b_0}{\lambda},\end{aligned}\quad (11)$$

The elliptic duct considered in this problem has hydraulic diameter given as

$$D_h = \frac{\pi b_0}{E(e)}, \quad (12)$$

In Eq. (12) $e = \sqrt{1 - \delta^2}$ is ellipse eccentricity and $E(e)$ (i.e. elliptic integral of 2nd kind) is provided by [28].

$$E(e) = \int_0^{\pi/2} \sqrt{1 - e^2 \text{Sin}^2 \alpha_1} d\alpha_1, \quad (13)$$

First using Eq. (10) and then the dimensionless variables provided in Eq. (11) in Eqs. (4–8), finally the simplified partial differential equations that govern the flow and heat transfer are achieved by using the long wavelength ($\lambda \rightarrow \infty$).

$$\frac{\partial p}{\partial x} = 0, \quad (14)$$

$$\frac{\partial p}{\partial y} = 0, \quad (15)$$

$$\frac{dp}{dz} = \frac{\partial^2 w}{\partial x^2} + \frac{\partial^2 w}{\partial y^2}, \quad (16)$$

$$\frac{\partial^2 \theta}{\partial x^2} + \frac{\partial^2 \theta}{\partial y^2} + B_r \left[\left(\frac{\partial w}{\partial x} \right)^2 + \left(\frac{\partial w}{\partial y} \right)^2 \right] = 0, \quad (17)$$

With following non-dimensional mathematical conditions over the boundary of elliptic duct having ciliated walls are defined as

$$w = -1 - \frac{2\pi\phi\alpha\beta\text{Cos}(2\pi z)}{1 - 2\pi\phi\alpha\beta\text{Cos}(2\pi z)}, \text{ for } \frac{x^2}{a^2} + \frac{y^2}{b^2} = 1. \quad (18)$$

$$\theta = 0, \text{ for } \frac{x^2}{a^2} + \frac{y^2}{b^2} = 1, \quad (19)$$

The values of a and b are given as

$$a = \frac{E(e)}{\pi} \left[\frac{1}{\delta} + \phi \text{Sin}(2\pi z) \right], b = \frac{E(e)}{\pi} [1 + \phi \text{Sin}(2\pi z)]$$

3. Exact solution

We have considered a polynomial type solution of the velocity profile given as

$$w(x, y) = C_1 x^4 + C_2 y^4 + C_3 x^2 y^2 + C_4 x^2 + C_5 y^2 + C_6, \quad (20)$$

After using this polynomial expression for velocity profile in Eq. (16), we get following three equations by comparing coefficients of x^2, y^2, x^0, y^0

$$12C_1 + 2C_3 = 0,$$

$$2C_3 + 12C_2 = 0,$$

$$2C_4 + 2C_5 = \frac{dp}{dz},$$

Further using the polynomial expression given in Eq. (20) in the corresponding boundary condition provided in Eq. (18) and comparing coefficients of x^4, x^2, x^0 , we get these three equations

$$C_1 a^4 + C_2 b^4 - C_3 a^2 b^2 = 0,$$

$$-2C_2 b^4 + C_3 a^2 b^2 + C_4 a^2 - C_5 b^2 = 0,$$

$$C_2 b^4 + C_5 b^2 + C_6 = -1 - \frac{2\pi\phi\alpha\beta\text{Cos}(2\pi z)}{1 - 2\pi\phi\alpha\beta\text{Cos}(2\pi z)},$$

These are six equations ($i - vi$) with six constants and we have solved these equations simultaneously to get values of these constants given as

$$\begin{aligned}C_1 &= 0, C_2 = 0, C_3 = 0, C_4 = \frac{b^2 \frac{dp}{dz}}{2(a^2 + b^2)}, C_5 \\ &= \frac{a^2 \frac{dp}{dz}}{2(a^2 + b^2)}, C_6 \\ &= -\frac{a^2 b^2 \frac{dp}{dz}}{2(a^2 + b^2)} + \frac{1}{2\pi\phi\alpha\beta\text{Cos}(2\pi z) - 1},\end{aligned}\quad (21)$$

These constants given in Eq. (21) are substituted in Eq. (20) and here is the simplified form of velocity solution that exactly satisfies Eq. (16) and the relevant conditions (18) over the boundary of elliptic duct having ciliated walls

$$\begin{aligned}w(x, y) &= -1 - \frac{2\pi\phi\alpha\beta\text{Cos}(2\pi z)}{1 - 2\pi\phi\alpha\beta\text{Cos}(2\pi z)} + \frac{1}{2} \frac{a^2 b^2}{(a^2 + b^2)} \\ &\quad \times \frac{dp}{dz} \left(\frac{x^2}{a^2} + \frac{y^2}{b^2} - 1 \right),\end{aligned}\quad (22)$$

The dimensionless flow rate $q(z)$ is calculated by integrating velocity Eq. (22) over an elliptic cross section

$$q(z) = -\frac{a^3 b^3 \left(\frac{dp}{dz} \right) \pi}{4(a^2 + b^2)} + \frac{ab\pi}{-1 + 2\pi\phi\alpha\beta\text{Cos}(2\pi z)}, \quad (23)$$

The mathematical result of pressure gradient is obtained by using Eq. (23)

$$\frac{dp}{dz} = \frac{4(a^2 + b^2) \left(\frac{\int_0^1 abdz - Q}{\pi} + \frac{ab}{-1 + 2\pi\phi z\beta \cos(2\pi z)} \right)}{a^3 b^3}, \quad (24)$$

The pressure rise for one wavelength is obtained by

$$\Delta P = \int_0^1 \frac{\partial p}{\partial z} dz, \quad (25)$$

Now adopting the same manner that is utilized to get velocity solution, we get this exact temperature solution that satisfy both Eqs. (17) and (19)

$$\theta(x,y) = \frac{-a^2 b^2 B_r \left(\frac{dp}{dz} \right)^2 \left(\frac{x^2 + y^2}{a^2 + b^2} - 1 \right) [b^6 x^2 + a^2 b^4 (b^2 + 6x^2 - y^2) + a^6 (b^2 + y^2) + a^4 b^2 (4b^2 - x^2 + 6y^2)]}{12(a^2 + b^2)^2 (a^4 + 6a^2 b^2 + b^4)} \quad (26)$$

4. Comparison with cylindrical ciliated tube

The present study is compared with a cylindrical ciliated tube [29] and the major observations are provided as follows

- An increase in the velocity profile is noted for both the ciliated ducts having elliptic or cylindrical cross-section with increasing Q .
- A parabolic flow profile is observed for both cases.
- A decline in the drag force is anticipated for an elliptic duct in comparison to a circular one.
- A lower pressure drop is observed for an elliptic duct in comparison to a circular one.
- An increase in the heat transfer coefficient is noted for an elliptic duct.

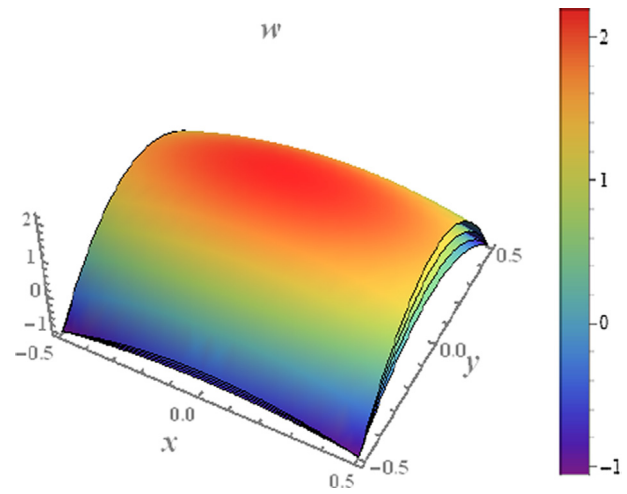


Fig. 3 (continued)

5. Result and discussion

For a better analysis of this present problem, we have presented the graphical assessment of results obtained in exact solution section. This section incorporates both 3D-plots as well as 2D-plots of velocity and temperature solutions. In Figs. 3-5, the graphical solutions are presented to interpret the flow behaviour for distinct values of dimensionless parameters. It is evident from these graphical results of velocity that the flow behaviour in this elliptic duct is axial symmetric flow. Further, a maximum value of velocity profile is observed in the

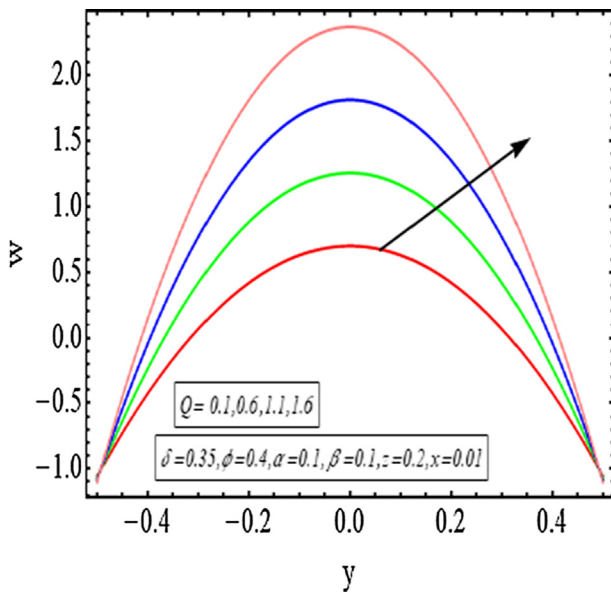


Fig. 3 (a) velocity plot for Q (2-dimensional). (b) velocity plot for Q (3-dimensional).

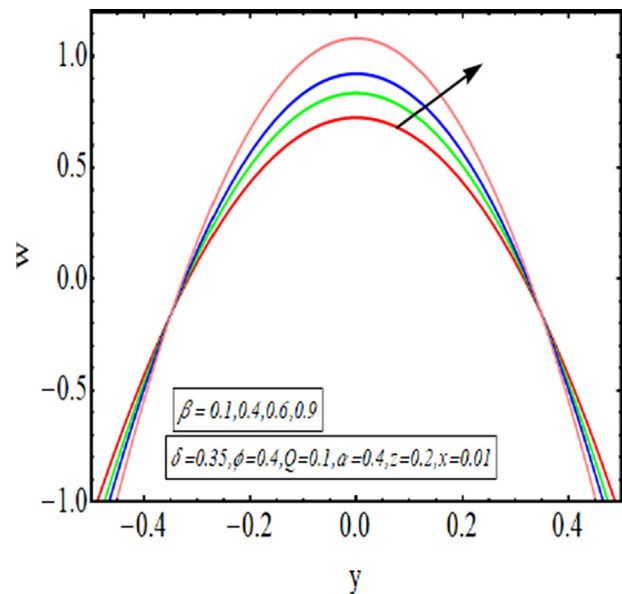


Fig. 4 (a) velocity plot for β (2-dimensional) (b) velocity plot for β (3-dimensional)..

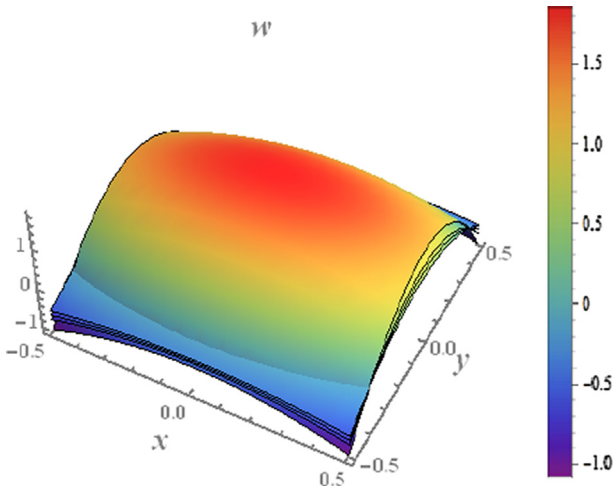


Fig. 4 (continued)

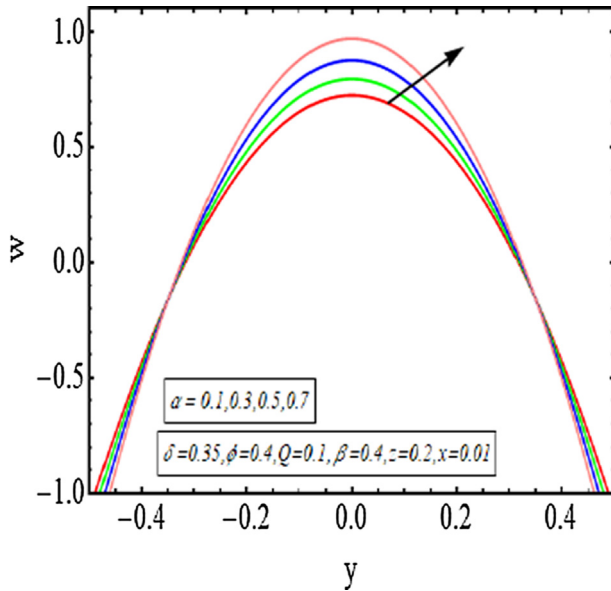


Fig. 5 (a) velocity plot for α (2-dimensional). (b) velocity plot for α (3-dimensional).

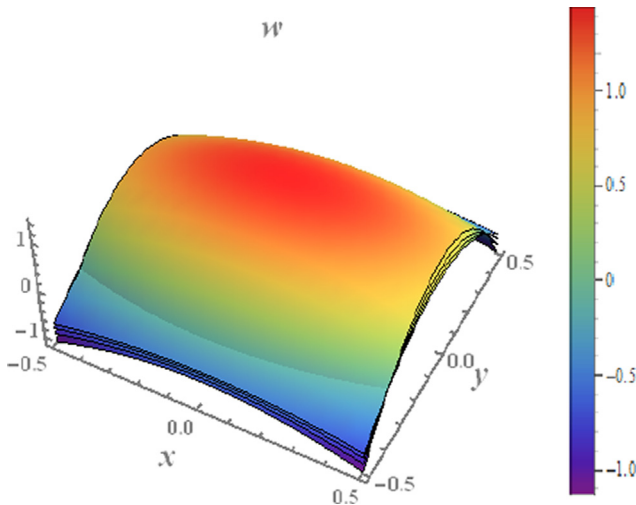


Fig. 5 (continued)

middle of this elliptic duct and it gradually decreases toward the ciliated walls of elliptic duct. Thus an axially symmetry flow behaviour is observed for peristaltic flow in an elliptic duct having ciliated walls. Fig. 3 provides the velocity behaviour for increasing Q and it is clear from Fig. 3(a) (a 2-dimensional velocity plot) that velocity is an increasing function of Q . The 3D-plot of velocity for increasing Q is given in Fig. 3(b) and it is evident that velocity is low at the walls of duct while it gains maximum value in the centre of duct. Fig. 4 depicts the graphical result of velocity for distinct values of wave number β . Fig. 4(a) shows that velocity is here an increasing function of wave number. Since a rise in the flow is observed in the middle of duct for increasing β but an opposing behaviour is noted towards the walls of ciliated duct. Fig. 4 (b) also shows this opposing behaviour of velocity at middle of duct and near ciliated walls. Since velocity is increasing in the middle of duct and eventually gains maximum value but at the same time it is declining near ciliated walls of duct. Fig. 5 reveals that velocity is also an increasing function of α . It unfolds that the increasing eccentricity of the elliptic motion of cilia also increases the main flow. Both the Fig. 5(a) (2-D plot) and (5b) (3D-plot) depicts an increasing velocity in the centre of duct but declining velocity near ciliated walls of duct. Figs. 6-9 are presented to analyse the flow of heat in this ciliated elliptic duct having sinusoidal walls. Here again an axial symmetry heat transfer is observed just like velocity profile. Also it is depicted by these graphs of temperature that temperature is high in the middle of duct and it decreases smoothly towards the walls and becomes zero. Thus the flow of heat in an elliptic duct having ciliated walls is axially symmetric. Fig. 6 depicts the flow of heat for increasing Q and it is disclosed from Fig. 6(a) that temperature is an increasing function of Q . Fig. 6(b) shows maximum temperature at the centre of duct and it declines smoothly towards ciliated walls of elliptic duct. Fig. 7 is plotted to analyse the effect of B_1 ,

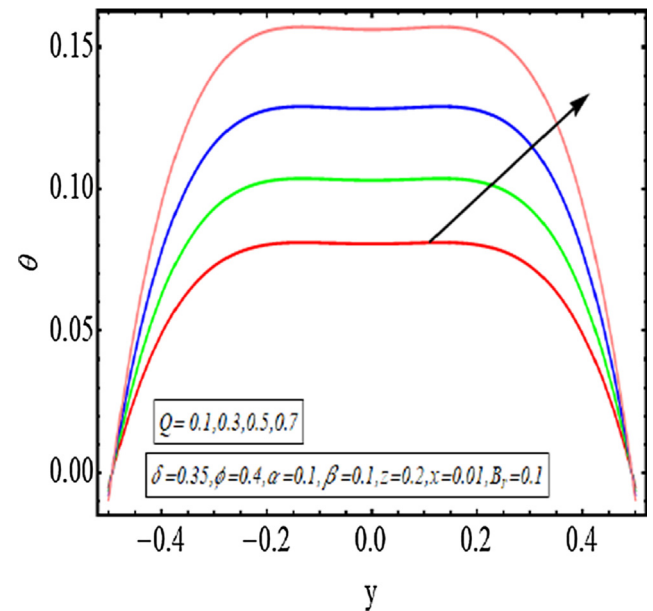


Fig. 6 (a) Temperature plot for Q (2-dimensional). (b) Temperature plot for Q (3-dimensional).

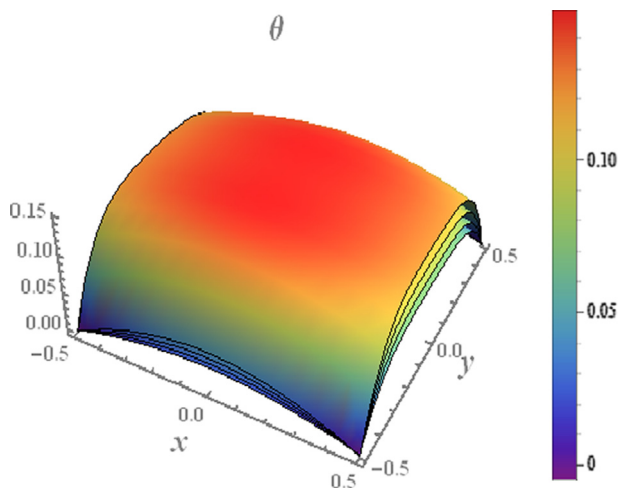


Fig. 6 (continued)

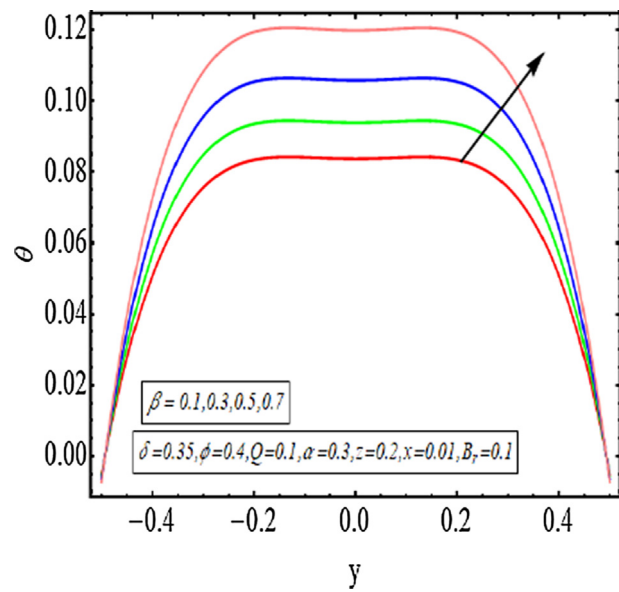


Fig. 8 (a) Temperature plot for β (2-dimensional). (b) Temperature plot for β (3-dimensional).

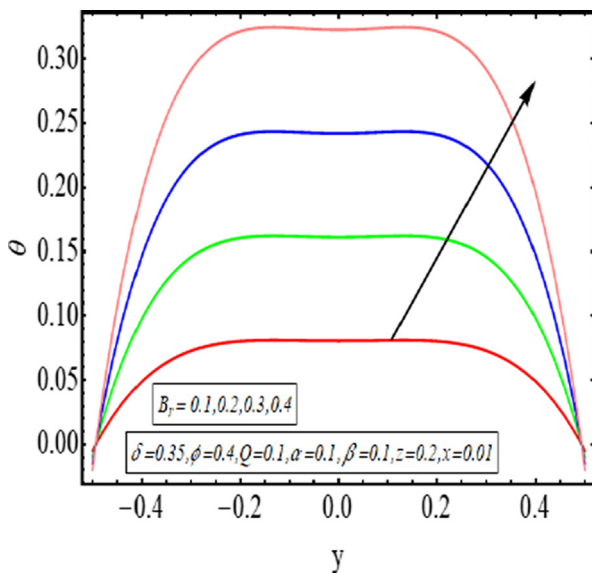


Fig. 7 (a) Temperature plot for B_r (2-dimensional). (b) Temperature plot for B_r (3-dimensional).

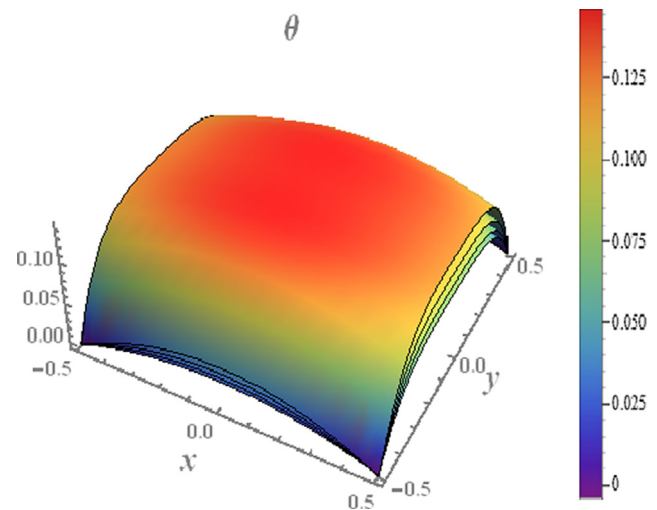


Fig. 8 (continued)

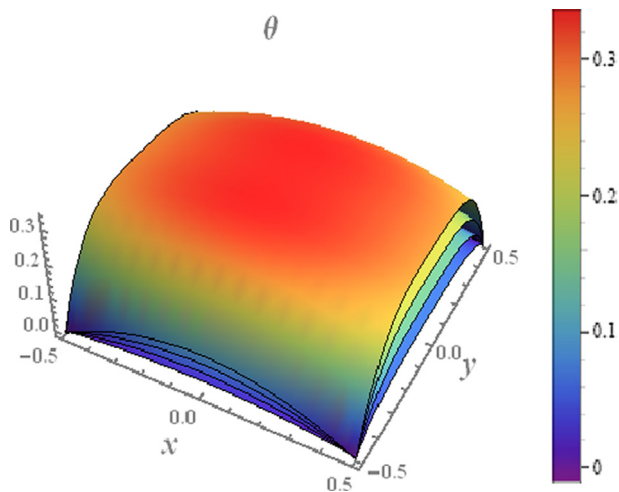


Fig. 7 (continued)

on temperature profile. It is noted in Fig. 7(a) that temperature is an increasing function of B_r . Fig. 7(b) displays that the flow of heat is high at the middle of duct and decreases towards walls. Fig. 8 depicts the effect of β on flow of heat. It is evident from Fig. 8(a) that temperature is an increasing function of β . The heat transfer rate is maximum in the central region of this elliptic duct and minimum at the ciliated walls, as shown in Fig. 8(b). Fig. 9 provides the effect of α on temperature profile and it is clearly observed in Fig. 9(a) that temperature is an increasing function of α . That is the eccentricity of elliptic motion of cilia play a vital role in the enhancement of the flow temperature. Further, Fig. 9(b) shows a maximum temperature in the centre that gradually decreases and becomes zero at the ciliated walls. The temperature graphical outcomes reveal that

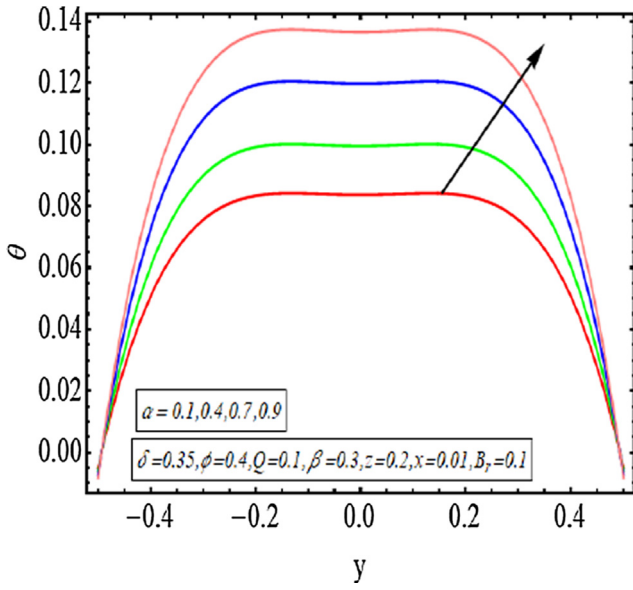


Fig. 9 (a) Temperature plot for α (2-dimensional). (b) Temperature plot for α (3-dimensional).

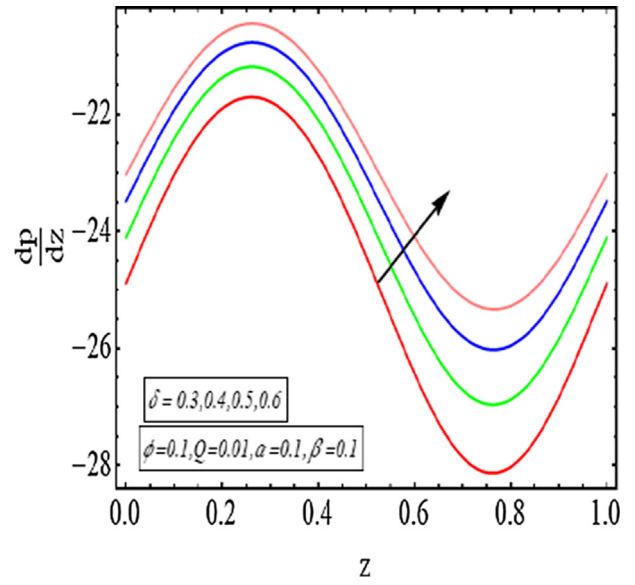


Fig. 10 (a) $\frac{dp}{dz}$ for δ . (b) $\frac{dp}{dz}$ for ϕ . (c) $\frac{dp}{dz}$ for Q .

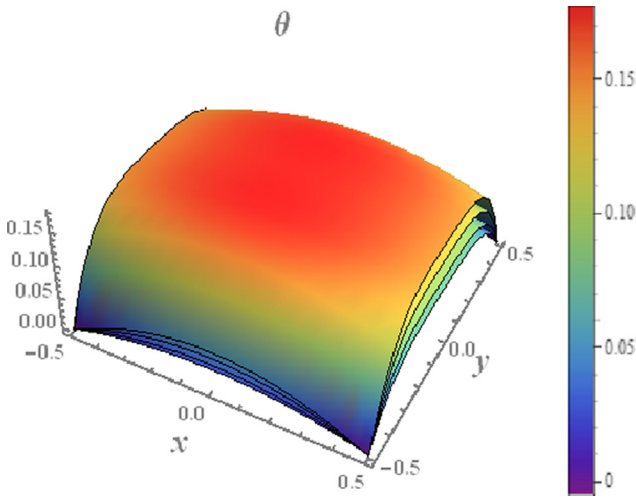


Fig. 9 (continued)

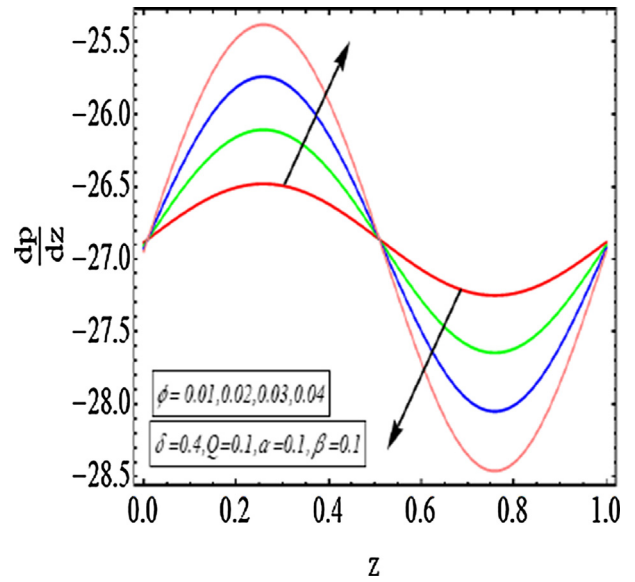


Fig. 10 (continued)

the coefficient of heat transfer has increased for the case of an elliptic duct. Fig. 10(a-c) are the graphical solutions of pressure gradient that are plotted against axial coordinate. Fig. 10(a) depicts that $\frac{dp}{dz}$ is an increasing function of δ . It is evident from Fig. 10(b) that $\frac{dp}{dz}$ is an increasing function of ϕ for $0 \leq z \leq 0.5$ while at the same time it is decreasing function of ϕ for $0.5 \leq z \leq 1$. Thus there a rise in the value of pressure gradient for an expanding sinusoidal wave but at the same time it declines for a contracting sinusoidal wave at the elliptic duct walls.

Further, this decline in the pressure gradient eventually assists the flow and thus the fluid is propelled along the axial coordinate of duct due to contraction of peristaltic wave. Fig. 10(c) reveals that $\frac{dp}{dz}$ is a decreasing function of Q . In Fig. 11 (a-b), the graphical solutions of ΔP are plotted against Q . The elliptic duct has a lower pressure drop as compared to the circular

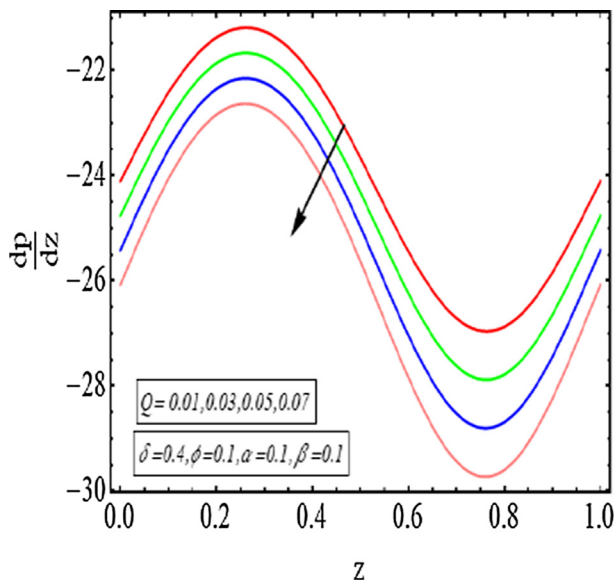


Fig. 10 (continued)

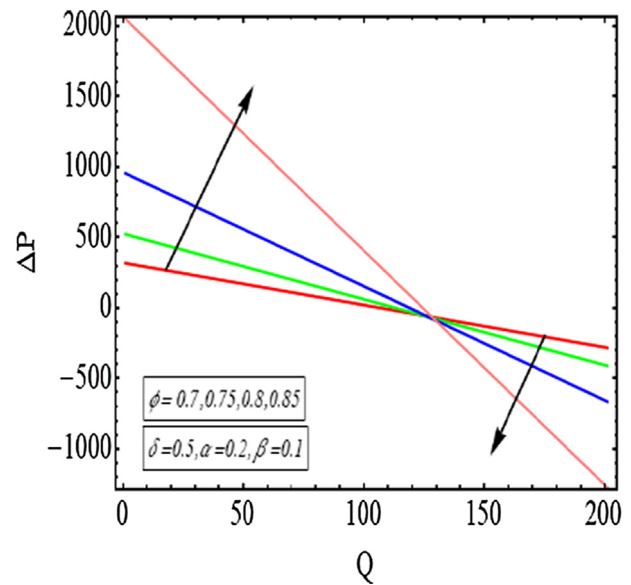


Fig. 11 (continued)

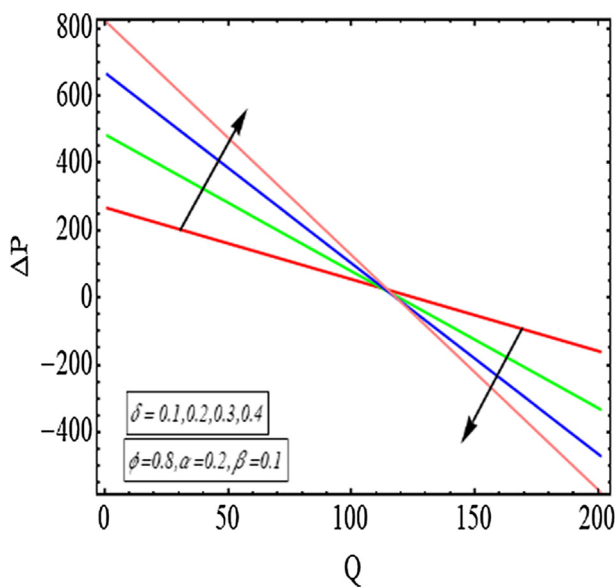


Fig. 11 (a) ΔP against Q for δ . (b) ΔP against Q for ϕ .

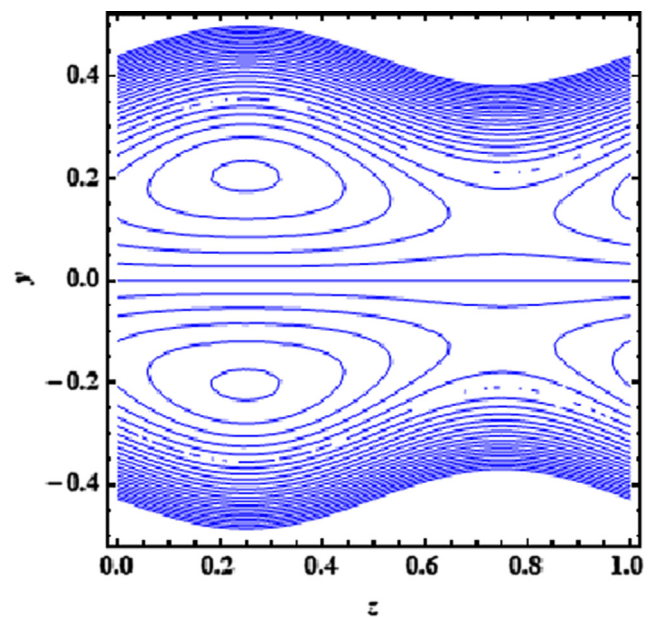


Fig. 12 (a) Streamlines plot for $Q = 0.01$. (b) Streamlines plot for $Q = 0.03$. (c) Streamlines plot for $Q = 0.05$. (d) Streamlines plot for $Q = 0.07$.

duct. Fig. 11(a) depicts that ΔP is an increasing function of δ in the peristaltic pumping region while it is decreasing a function of δ in the co-pumping segment. Similarly, Fig. 11(b) depicts that ΔP is varying directly with ϕ in the peristaltic pumping section while it varies inversely with ϕ in the co-pumping region. In Fig. 12(a-d), the graphical results are presented for

streamlines. These streamlines depict a side-view of flow in this elliptic duct. It is revealed that the closed contours are increasing in size with increasing flow rate.

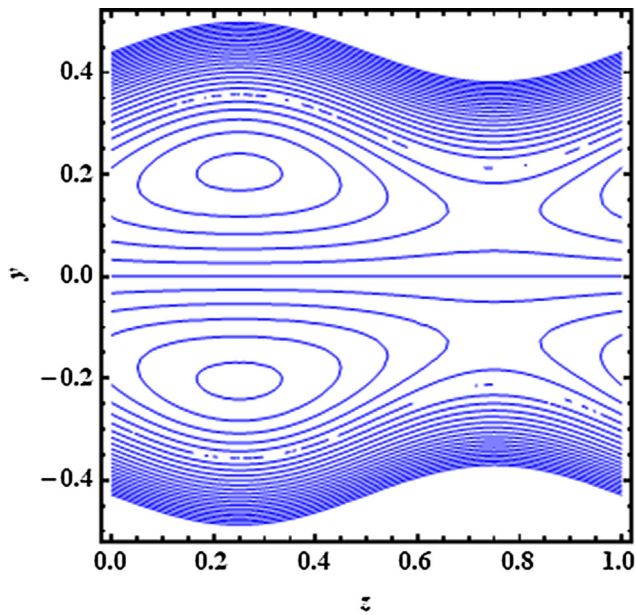


Fig. 12 (continued)

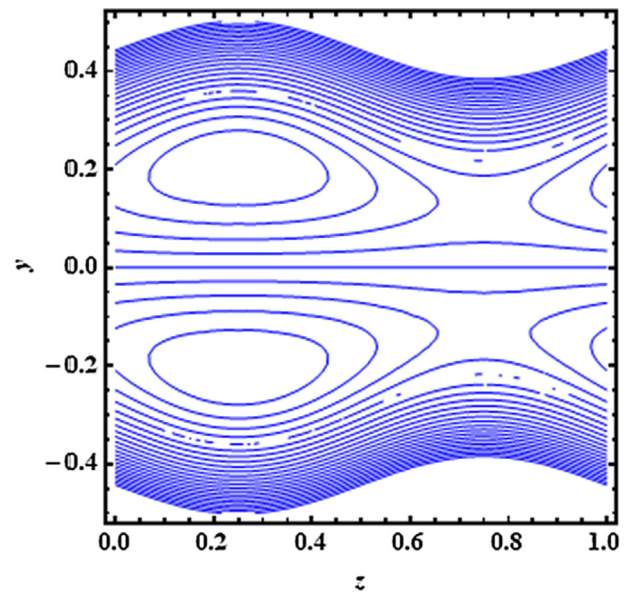


Fig. 12 (continued)

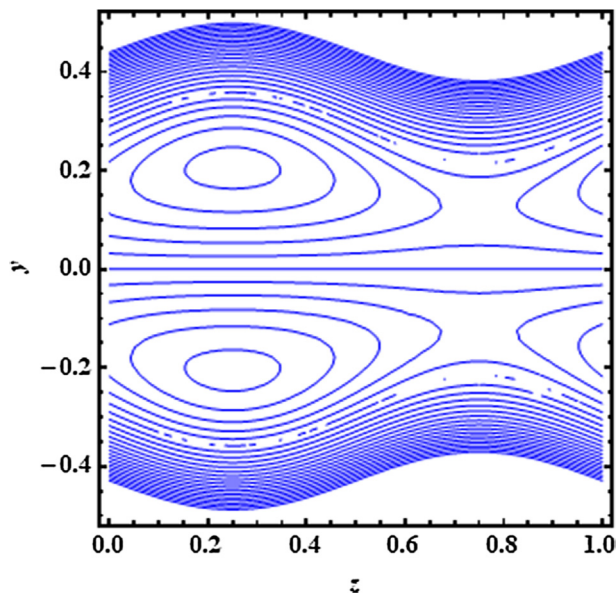


Fig. 12 (continued)

6. Conclusions

The present problem is modelled for an elliptic duct with ciliated walls. We have conveyed a thorough analysis for flow of heat and various physical characteristics of peristaltic flow mechanism. Our motivation in this novel work was to combine the effects of peristalsis and cilia in a duct with elliptic cross-section. The key findings of our current investigation includes

- The exact solution section provides a complete methodology to solve the partial differential equations with boundary conditions over the surface of an ellipse having ciliated walls.
- It is evident from the graphical results of velocity that the flow behaviour in this elliptic duct is axial symmetric flow.
- A maximum value of velocity profile is observed in the middle of this elliptic duct and it gradually decreases toward the ciliated walls of elliptic duct.
- The flow of heat in an elliptic duct having ciliated walls is axially symmetric.
- Temperature is high in the middle of duct and it decreases smoothly towards the walls and becomes zero.
- The streamlines depict a side-view of flow in this elliptic duct. It is noted that the closed contours are increasing in size with incrementing value of Q .

CRedit authorship contribution statement

L.B. McCash: Conceptualization, Funding. **Salman Akhtar:** Data curation, Writing- Original draft preparation, Investigation. **Sohail Nadeem:** Supervision, Visualization. **Anber Saleem:** Software. **Salman Saleem:** Writing - reviewing and editing. **Alibek Issakhov:** Validation, Methodology.

Declaration of Competing Interest

The authors declare that they have no known competing financial interests or personal relationships that could have appeared to influence the work reported in this paper.

Acknowledgements

The authors extend their appreciation to the Deanship of Scientific Research at King Khalid University for funding this work through research groups program under Grant No. RGP.1/183/42.

References

- [1] M.Y. Jaffrin, A.H. Shapiro, Peristaltic pumping, *Annu. Rev. Fluid Mech.* 3 (1) (1971) 13–37.
- [2] C. Barton, S. Raynor, Peristaltic flow in tubes, *The Bulletin of mathematical biophysics* 30 (4) (1968) 663–680.
- [3] C. Pozrikidis, A study of peristaltic flow, *J. Fluid Mech.* 180 (-1) (1987) 515, <https://doi.org/10.1017/S0022112087001939>.
- [4] A.M. Siddiqui, W.H. Schwarz, Peristaltic flow of a second-order fluid in tubes, *J. Nonnewton. Fluid Mech.* 53 (1994) 257–284.
- [5] S. Nadeem, N.S. Akbar, Peristaltic flow of Sisko fluid in a uniform inclined tube, *Acta Mech. Sin.* 26 (5) (2010) 675–683.
- [6] S. Nadeem, E.N. Maraj, The mathematical analysis for peristaltic flow of hyperbolic tangent fluid in a curved channel, *Commun. Theor. Phys.* 59 (6) (2013) 729–736.
- [7] S. Nadeem, S. Akram, Peristaltic flow of a Williamson fluid in an asymmetric channel, *Commun. Nonlinear Sci. Numer. Simul.* 15 (7) (2010) 1705–1716.
- [8] Akram, S., & Saleem, N. (2020). Analysis of Heating Effects and Different Wave Forms on Peristaltic Flow of Carreau Fluid in Rectangular Duct. *Advances in Mathematical Physics*, 2020.
- [9] A. Saleem, S. Akhtar, S. Nadeem, F.M. Alharbi, M. Ghalambaz, A. Issakhov, Mathematical computations for Peristaltic flow of heated non-Newtonian fluid inside a sinusoidal elliptic duct, *Phys. Scr.* 95 (10) (2020) 105009, <https://doi.org/10.1088/1402-4896/abb3>.
- [10] Huang, Y. M., & Ho, C. H. (1993). Study of the Fluid Flow in the Elliptical Duct by the Method of Characteristics.
- [11] R.M. Abdel-Wahed, A.E. Attia, M.A. Hifni, Experiments on laminar flow and heat transfer in an elliptical duct, *Int. J. Heat Mass Transf.* 27 (12) (1984) 2397–2413.
- [12] C.R.M. Maia, J.B. Aparecido, L.F. Milanez, Heat transfer in laminar flow of non-Newtonian fluids in ducts of elliptical section, *Int. J. Therm. Sci.* 45 (11) (2006) 1066–1072.
- [13] H. Ragueb, K. Mansouri, A numerical study of viscous dissipation effect on non-Newtonian fluid flow inside elliptical duct, *Energy Convers. Manage.* 68 (2013) 124–132.
- [14] H. Ragueb, K. Mansouri, An analytical study of the periodic laminar forced convection of non-Newtonian nanofluid flow inside an elliptical duct, *Int. J. Heat Mass Transf.* 127 (2018) 469–483.
- [15] S. Mir, O.A. Akbari, D. Toghraie, G. Sheikhzadeh, A. Marzban, S. Mir, P. Talebizadehsardari, A comprehensive study of two-phase flow and heat transfer of water/Ag nanofluid in an elliptical curved minichannel, *Chin. J. Chem. Eng.* 28 (2) (2020) 383–402.
- [16] Etaig, S., & Hashem, G. Numerical Investigation on the Laminar Flow in a Vertical Pipe with Elliptic Cross Section.
- [17] T.J. Lardner, W.J. Shack, Cilia transport, *The bulletin of mathematical biophysics* 34 (3) (1972) 325–335.
- [18] J. Blake, Flow in tubules due to ciliary activity, *Bull. Math. Biol.* 35 (4) (1973) 513–523.
- [19] N. Sher Akbar, Z.H. Khan, Heat transfer study of an individual multiwalled carbon nanotube due to metachronal beating of cilia, *Int. Commun. Heat Mass Transfer* 59 (2014) 114–119.
- [20] N.S. Akbar, A.W. Butt, Heat transfer analysis of viscoelastic fluid flow due to metachronal wave of cilia, *International Journal of Biomathematics* 07 (06) (2014) 1450066, <https://doi.org/10.1142/S1793524514500661>.
- [21] N. Sher Akbar, Biomathematical analysis of carbon nanotubes due to ciliary motion, *International Journal of Biomathematics* 08 (02) (2015) 1550023, <https://doi.org/10.1142/S1793524515500230>.
- [22] A.W. Butt, N.S. Akbar, N.A. Mir, Heat transfer analysis of peristaltic flow of a Phan-Thien–Tanner fluid model due to metachronal wave of cilia, *Biomech. Model. Mechanobiol.* 19 (5) (2020) 1925–1933.
- [23] A. Saleem, S. Akhtar, F.M. Alharbi, S. Nadeem, M. Ghalambaz, A. Issakhov, Physical aspects of peristaltic flow of hybrid nano fluid inside a curved tube having ciliated wall, *Results Phys.* 19 (2020) 103431, <https://doi.org/10.1016/j.rinp.2020.103431>.
- [24] A.Z. Zaher, A.M.A. Moawad, K.S. Mekheimer, M.M. Bhatti, Residual time of sinusoidal metachronal ciliary flow of non-Newtonian fluid through ciliated walls: fertilization and implantation, *Biomech. Model. Mechanobiol.* 20 (2) (2021) 609–630.
- [25] R.E. Abo-Elkhair, M.M. Bhatti, K.S. Mekheimer, Magnetic force effects on peristaltic transport of hybrid bio-nanofluid (AuCu nanoparticles) with moderate Reynolds number: An expanding horizon, *Int. Commun. Heat Mass Transfer* 123 (2021) 105228, <https://doi.org/10.1016/j.icheatmasstransfer.2021.105228>.
- [26] M.M. Bhatti, A. Riaz, L. Zhang, S.M. Sait, R. Ellahi, Biologically inspired thermal transport on the rheology of Williamson hydromagnetic nanofluid flow with convection: an entropy analysis, *J. Therm. Anal. Calorim.* (2020) 1–16.
- [27] Zhang, L., Bhatti, M. M., Marin, M., & S Mekheimer, K. (2020). Entropy analysis on the blood flow through anisotropically tapered arteries filled with magnetic zinc-oxide (ZnO) nanoparticles. *Entropy*, 22(10), 1070.
- [28] Z.H. Yang, Y.M. Chu, W. Zhang, Monotonicity of the ratio for the complete elliptic integral and Stolarsky mean, *Journal of Inequalities and Applications* 2016 (1) (2016) 1–10.
- [29] N.S. Akbar, A.W. Butt, D. Tripathi, O.A. Béq, Physical hydrodynamic propulsion model study on creeping viscous flow through a ciliated porous tube, *Pramana* 88 (3) (2017) 52.